THE CHIRAL LONG-RANGE TWO-PION EXCHANGE ELECTROMAGNETIC CURRENTS IN RADIATIVE NUCLEON–DEUTERON CAPTURE

R. Skibiński, J. Golak, D. Rozpędzik, K. Topolnicki, H. Witała

The Marian Smoluchowski Institute of Physics, Jagiellonian University
Łojasiewicza 11, 30-348, Kraków, Poland

(Received December 8, 2014)

The nucleon–deuteron radiative capture process is investigated using the chiral nuclear potentials and the electromagnetic currents developed by the Bochum–Bonn group. While the strong interaction is taken up to the next-to-next-to-leading order, the electromagnetic current consists of a single nucleon current, the leading one-pion exchange one and is supplemented by contributions from the long-range two-pion exchange current at next-to-leading-order. The theoretical predictions for the cross sections as well as analyzing powers show strong dependence on the values of regularization parameters. Only small effects of the three-nucleon force and the long-range two-pion exchange current are observed. The dependence on the choice of regularization parameters results in a big theoretical uncertainty and clearly points to the necessity to include corrections from higher orders of the chiral expansion both for the nuclear forces and currents.

DOI:10.5506/APhysPolB.46.159
PACS numbers: 25.20.–x, 21.30.–x, 21.45.+v, 24.70.+s

1. Introduction

In the recent decade, the chiral Effective Field Theory (χEFT) has proven its predictive power in low energy nuclear physics. In the nucleon/pion sector, it was successfully applied to such processes as pion–nucleon scattering, nucleon–nucleon scattering, three-nucleon reactions and to the analysis of heavier systems. For a review on the χEFT and its recent applications, see *e.g.* [1–3]. Among many theoretical advantages of the χEFT, the consistency of the derived two- and three-body forces and interrelated single and many-body electromagnetic and week currents should be mentioned. This predisposes the χEFT to be used in studies of electromagnetic processes.

On the other hand, the inclusion of the electromagnetic current can be done also in an approximate way by means of the Siegert theorem [4]. Both approaches lead to similar results for proton–deuteron (pd) capture and for photodisintegration processes [5, 6]. In this work, we extend the results of [7] by using explicitly the chiral electromagnetic current instead of the Siegert approach. We follow here the path charted in [8] and use the single nucleon current, the leading one-pion exchange current and the next-to-leading order (NLO) contributions to the long-range part of the two-pion (2π) exchange current. In [8], the effects of the 2π-exchange currents were explored mainly in the deuteron photodisintegration reaction. It was found that the long-range 2π-exchange current operator plays an important role for that process.

In the next section, we briefly present our formalism for the nucleon–deuteron radiative capture and give details on the electromagnetic current. In Sec. 3 we present predictions for pd-capture at two laboratory energies of the incoming deuteron: 17.5 MeV and 137 MeV. These deuteron energies correspond to photon energies 11.3 and 50.4 MeV in the centre-of-mass system, respectively. We conclude in Sec. 4.

2. Theoretical description of the radiative Nd-capture reaction

The radiative pd-capture process $p+d \to \gamma+{}^3\mathrm{He}$ is connected to the two-body photodisintegration of ${}^3\mathrm{He}$ via the time reversal symmetry. Thus we obtain the nuclear matrix elements N_μ^{rad} for the radiative nucleon–deuteron (Nd) capture reaction from the matrix elements $N_\mu^{Nd} \equiv \langle \Psi_{Nd}^{(-)} \mid j_\mu \mid \Psi_b \rangle$ for the photodisintegration process. The N_μ^{Nd} can be expressed as

$$N_\mu^{Nd} = \langle \phi_1 \mid (1+P) \mid j_\mu \mid \Psi_b \rangle + \langle \phi_1 \mid P \mid \tilde{U} \rangle \,, \tag{1}$$

where $|\,\phi_1\rangle$ is a product of the deuteron state and a momentum eigenstate of the spectator nucleon. Further, the $|\,\Psi_b\rangle$ is the initial three nucleon ($3N$) bound state, j_μ is the μ-component of the electromagnetic current operator and $P \equiv P_{12}P_{23} + P_{13}P_{23}$ is the permutation operator with two-body permutations P_{ij} interchanging the i^{th} and j^{th} nucleons.

The auxiliary state $|\,\tilde{U}\rangle$ fulfills the Faddeev-like equation [9]

$$\begin{aligned} \left|\tilde{U}\right\rangle \;=\; & \left(tG_0 + \tfrac{1}{2}(1+P)V_4^{(1)}G_0(tG_0+1)\right)(1+P)j_\mu \mid \Psi_b\rangle \\ & + \left(tG_0P + \tfrac{1}{2}(1+P)V_4^{(1)}G_0(tG_0+1)P\right) \mid \tilde{U}\rangle \,, \end{aligned} \tag{2}$$

where $V_4^{(1)}$ is a part of the $3N$ force which is symmetrical under the exchange of nucleons 2 and 3, G_0 is the free $3N$ propagator, and t is the t-matrix connected to the nucleon–nucleon (NN) interaction via the Lippmann–Schwinger equation.

We solve Eq. (2) in the momentum-space in the partial wave scheme. More details on our formalism and numerical performance can be found in [6, 9]. As the nuclear interaction, we use the NN and $3N$ potentials at the next-to-next-to-leading order ($\mathrm{N^2LO}$) developed by Epelbaum and collaborators in [10] and [11], respectively. These forces depend on two regularization parameters $(\Lambda, \tilde{\Lambda})$ used in the regularization of the Lippmann–Schwinger equation and three-nucleon force, and in the spectral function regularization of 2π exchanges in the chiral NN interaction [12]. The values of regularization parameters $(\Lambda, \tilde{\Lambda})$ are taken as in [11] and are listed below. We neglect the Coulomb interaction between protons in the initial proton–deuteron system. The nuclear electromagnetic current has been developed within the same approach and presented in [13, 14], and used in [8]. Here, we use the same current operator as in [8], where its structure and partial wave decomposition is discussed in detail.

3. Results

In Figs. 1–2, we show predictions obtained with a complete nuclear potential ($NN+3N$) at $\mathrm{N^2LO}$ and two models of the electromagnetic current. The light gray/blue band comprises predictions for different values of the regularization parameters $(\Lambda, \tilde{\Lambda})$ obtained with the single nuclear current and the leading one-pion exchange current. In predictions which contribute to the dark gray/magenta band also long-range corrections to the 2π-exchange current are included. In addition, Fig. 1 also shows the prediction based on the AV18 [15] NN force combined with the Urbana IX $3N$ force [16]. In this case, the electromagnetic current is a sum of the single nucleon current and two most important contributions to the meson exchange current: the so-called π-like and ρ-like terms [5]. At the lower energy $E_d = 17.5$ MeV, the differential cross section and both (the nucleon and the deuteron) vector analyzing powers are rather insensitive to the values of $(\Lambda, \tilde{\Lambda})$, what leads to relatively narrow bands. The predictions for tensor analyzing powers are much more sensitive to the values of the regularization parameters. The quality of the data [17, 18] description is similar for both models of electromagnetic current and only slight improvement is seen after inclusion of the NLO contributions. At the higher energy $E_d = 137$ MeV, all bands are much wider and no meaningful differences in predictions within two models of electromagnetic current are observed.

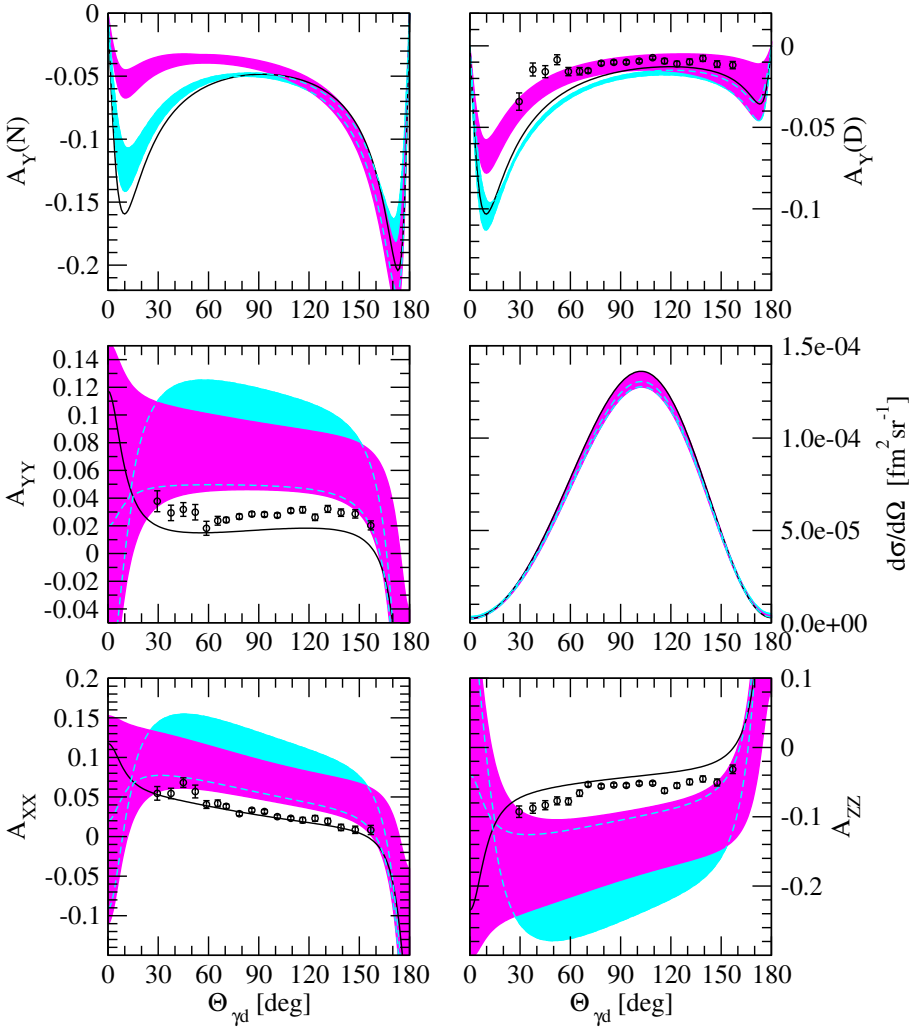

Fig. 1. The differential cross section and the analyzing powers for the proton–deuteron radiative capture at $E_d = 17.5$ MeV. The light gray/blue band corresponds to predictions which base on a single nucleon and one-pion exchange currents. The dark gray/magenta band corresponds to predictions which base on the same currents supplemented by the long-range 2π-exchange currents at NLO (see the text). The dashed line shows the borders of the lighter band. The solid black line is for the AV18+Urbana IX and the standard meson exchange currents (see the text) predictions. Experimental data points are taken from [17, 18].

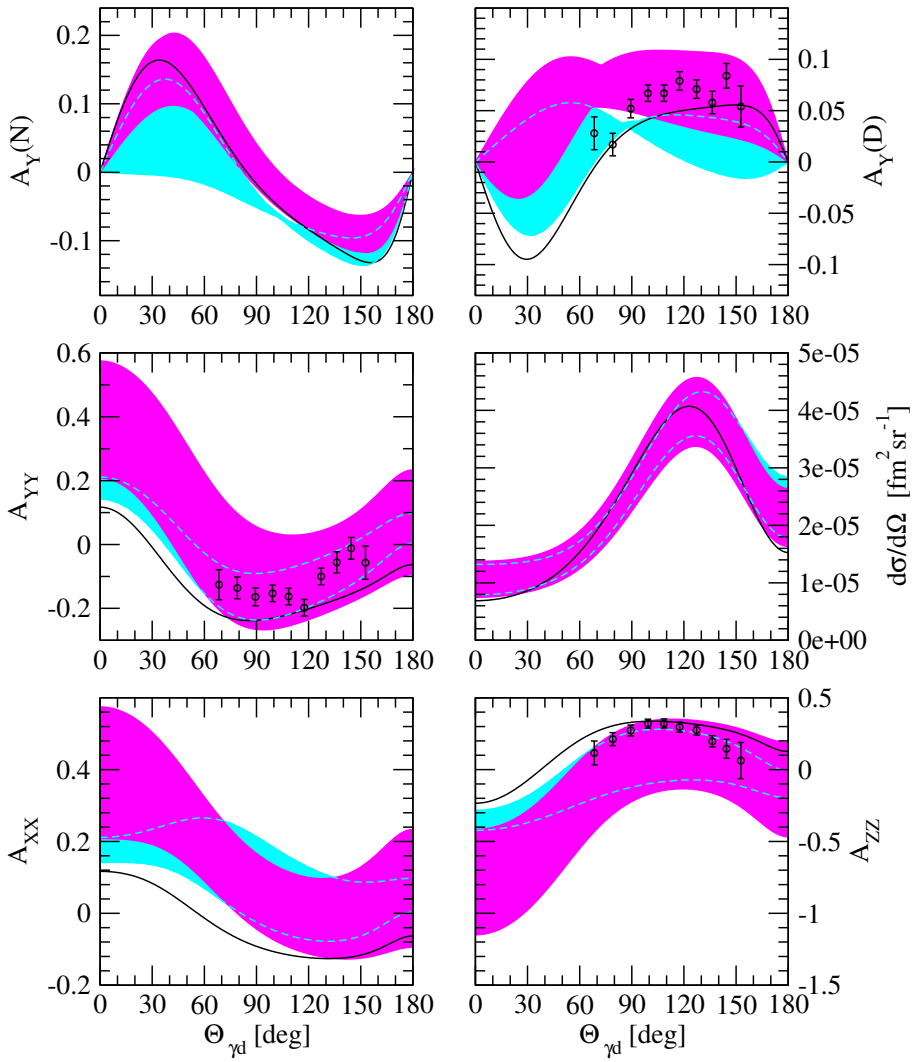

Fig. 2. The same as in Fig. 1 but for the deuteron laboratory energy $E_d = 137$ MeV. Experimental data points at $E_d = 133$ MeV are taken from [19].

In Fig. 3 we show in more detail the dependence of the predictions on the value of regularization parameters. The presented lines are the same that build the dark gray/magenta band in Fig. 1. The values of $(\Lambda, \tilde{\Lambda})$ are, in MeV: (450,500), (600,500), (550,600), (450,700), (600,700) for the dotted (black), double-dot-dashed (brown), dot-dashed (blue), dashed (magenta) and solid (red) curves, respectively. The strongest dependence is seen for the tensor analyzing powers. Note, that predictions based on the smallest values of Λ behave qualitatively similar to the reference predictions based

on the AV18+Urbana IX model, shown in Fig. 1. This is in agreement with recent findings in elastic Nd scattering at N^{3}LO where also the smallest values of Λ are favored [20].

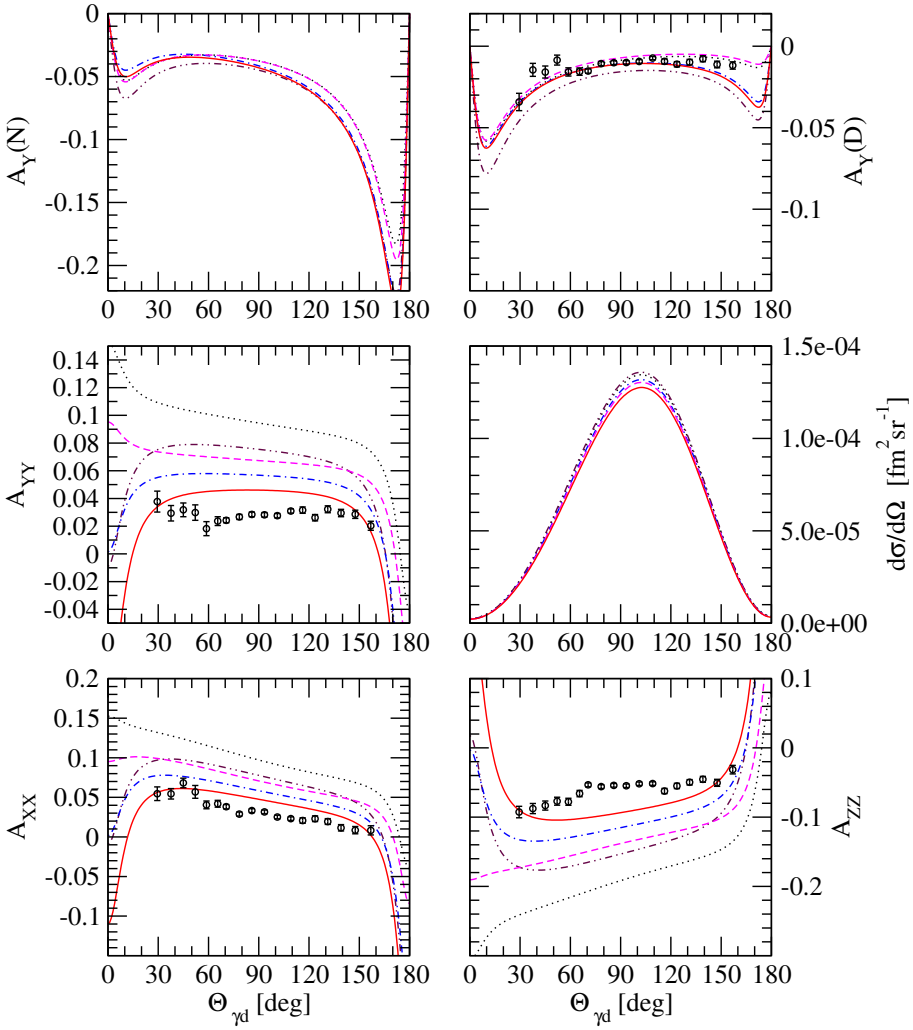

Fig. 3. The same as in Fig. 1 but now only contributions to the dark gray/magenta band are shown explicitly. Values of the $(\Lambda, \tilde{\Lambda})$ parameters are given in the text.

Finally, we test the sensitivity of the Nd-capture observables to the $3N$ force. In Fig. 4, we compare predictions based on the NN interaction only (light gray/blue band) with ones based on the full $NN + 3N$ Hamiltonian (dark gray/magenta band) for $E_d = 17.5$ MeV. The electromagnetic current operator is, again, taken as a sum of the single nucleon current, the one-

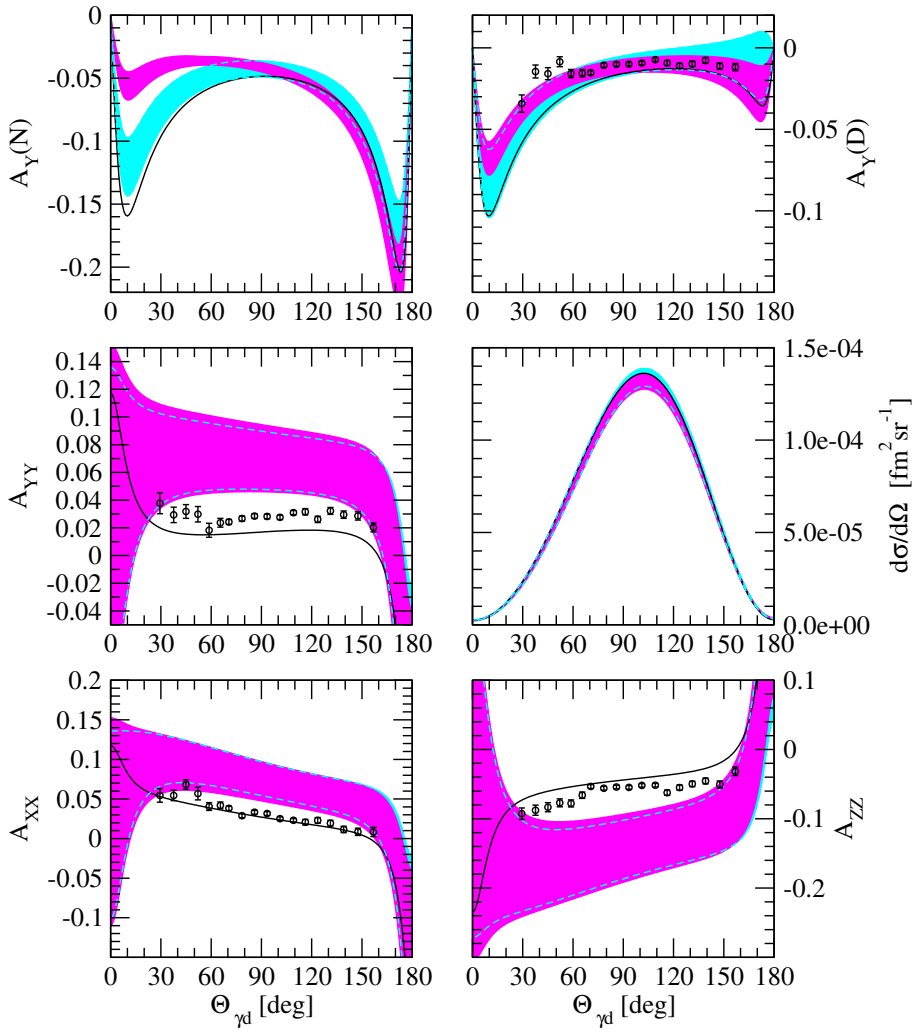

Fig. 4. The same as in Fig. 1 but now for predictions based on the NN N^{2}LO interaction only (light gray/blue band) and the full $NN + 3N$ Hamiltonian at N^{2}LO (dark gray/magenta band). The solid line and experimental data points are the same as in Fig. 1.

pion exchange current and the long-range 2π-exchange one. At this energy only predictions for the differential cross section and vector analyzing powers change after inclusion of the $3N$ force. However, this change is not big and comparable with the bands' width. For tensor analyzing powers, the $3N$ force effects are totally hidden by the dependence on the values of the regularization parameters. The latter is true also at $E_d = 137$ MeV (Fig. 5)

where, additionally, the $3N$ force effects are seen neither for the vector analyzing powers nor for the cross section. Again, for these dynamical models, the bands are too broad to be useful in a study of the $3N$ force effects.

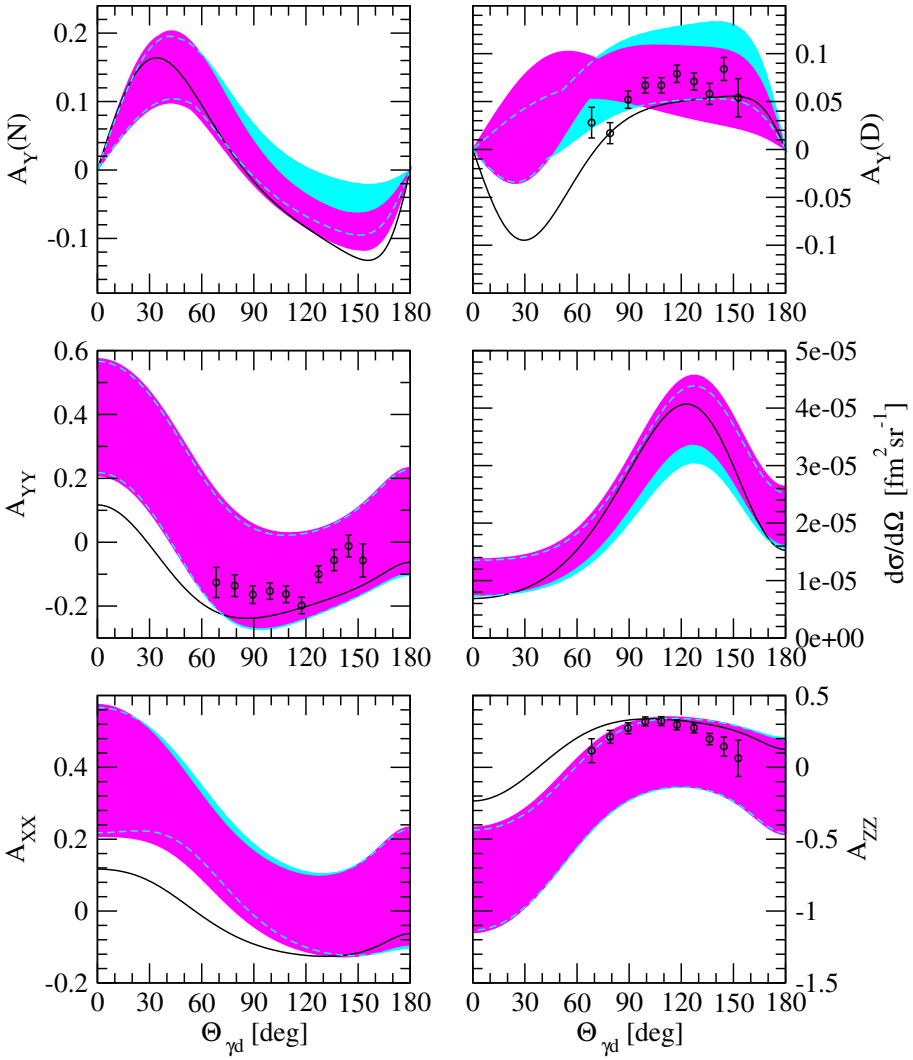

Fig. 5. The same as in Fig. 4 but for the deuteron laboratory energy $E_d = 137$ MeV. Experimental data points from [19] are taken at $E_d = 133$ MeV.

4. Summary

We have applied the chiral potential at N^{2}LO combined with the electromagnetic current taken as a sum of the single nucleon current, the one-pion exchange one and the long-range NLO part of the 2π-exchange current to study the differential cross section and the analyzing powers for the Nd radiative capture at deuteron energies 17.5 and 137 MeV.

For most observables, the effects of long-range 2π-exchange current at NLO as well as the effects of the $3N$ interaction at N^{2}LO are small compared to the uncertainty coming from different values of the regularization parameters. This clearly shows that a study of the Nd-capture reaction by means of χEFT requires consistent currents and interactions at higher orders of the chiral expansion. In addition, more constraints should be put on the values of the regularization parameters.

Recently, it was pointed that the dependence of the predictions for the Nd elastic scattering on the regularization parameters obtained within the χEFT at N^{3}LO also leads to unacceptably large theoretical uncertainties [20, 21]. It is expected that a new regularization scheme will cure such a situation [22]. Once it is available, it will be interesting to study the Nd-capture and other electromagnetic processes again. Such an investigation is planed in the future.

The authors would like to thank Prof. E. Epelbaum and Dr. S. Kölling for their help in the numerical realization of chiral interactions and current operators. This study was supported by the Polish National Science Center under Grants No. DEC-2013/10/M/ST2/00420 and DEC2013/11/N/ST2/03733. We acknowledge support by the Foundation for Polish Science — MPD program, co-financed by the European Union within the European Regional Development Fund. The numerical calculations have been performed on the supercomputer clusters of the JSC, Julich, Germany.

REFERENCES

[1] E. Epelbaum, *Prog. Part. Nucl. Phys.* **57**, 654 (2006).
[2] E. Epelbaum, H.-W.Hammer, U.-G. Meißner, *Rev. Mod. Phys.* **81**, 1773 (2009).
[3] R. Machleidt, D.R. Entem, *Phys. Rep.* **503**, 1 (2011).
[4] A. Siegert, *Phys. Rev.* **52**, 787 (1937).
[5] J. Golak *et al.*, *Phys. Rev.* **C62**, 054005 (2000).
[6] R. Skibiński *et al.*, *Phys. Rev.* **C67**, 054001 (2003).
[7] R. Skibiński *et al.*, *Acta Phys. Pol. B* **37**, 2905 (2006).

[8] D. Rozpędzik *et al.*, *Phys. Rev.* **C83**, 064004 (2011).
[9] J. Golak *et al.*, *Phys. Rep.* **415**, 89 (2005).
[10] E. Epelbaum, W. Glöckle, U.-G. Meißner, *Nucl. Phys.* **A747**, 362 (2005).
[11] E. Epelbaum *et al.*, *Phys. Rev.* **C66**, 064001 (2002).
[12] E. Epelbaum, W. Glöckle, U.-G. Meißner, *Eur. Phys. J.* **A19**, 125 (2004).
[13] S. Kölling, E. Epelbaum, H. Krebs, U.-G. Meißner, *Phys. Rev.* **C80**, 045502 (2009).
[14] S. Kölling, E. Epelbaum, H. Krebs, U.-G. Meißner, *Phys. Rev.* **C84**, 054008 (2011).
[15] R.B. Wiringa, V.G.J. Stoks, R. Schiavilla, *Phys. Rev.* **C51**, 38 (1995).
[16] J. Carlson, V.R. Pandpharipande, R.B. Wiringa, *Nucl. Phys.* **A401**, 59 (1983).
[17] K. Sagara *et al.*, *AIP Conf. Proc.* **334**, 467 (1995).
[18] H. Akiyoshi *et al.*, *Phys. Rev.* **C64**, 034001 (2001).
[19] A.A. Mehmandoost-Khajeh-Dad *et al.*, *Phys. Lett.* **B617**, 18 (2005).
[20] J. Golak *et al.*, *Eur. Phys. J.* **A50**, 177 (2014).
[21] H. Witała, J. Golak, R. Skibiński, K. Topolnicki, *J. Phys. G: Nucl. Part. Phys.* **41**, 094011 (2014).
[22] E. Epelbaum, private communication.